Michigan State University

National Superconducting Cyclotron Laboratory

MASS DEPENDENCE OF DIRECTED COLLECTIVE FLOW

M.J. HUANG, R.C. LEMMON, F. DAFFIN, W.G. LYNCH,
C. SCHWARTZ, M.B. TSANG, C. WILLIAMS,
P. DANIELEWICZ, K. HAGLIN, W. BAUER, N. CARLIN,
R.J. CHARITY, R.T. de SOUZA, C.K. GELBKE, W.C. HSI,
G.J. KUNDE, M-C. LEMAIRE, M.A. LISA, U. LYNEN,
G.F. PEASLEE, J. POCHODZALLA, H. SANN, L.G. SOBOTKA,
S.R. SOUZA, and W. TRAUTMANN

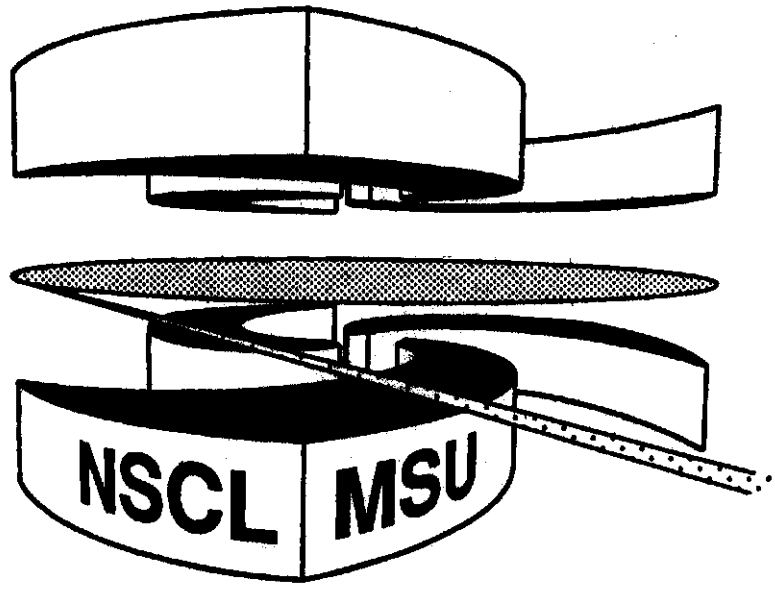

MSUCL-1044

SEPTEMBER 1996

Mass Dependence of Directed Collective Flow

M.J. Huang[a], R.C. Lemmon[a], F. Daffin[a], W.G. Lynch[a], C. Schwarz[ad], M.B. Tsang[a], C. Williams[a], P. Danielewicz[a], K. Haglm', W. Bauer[a], N. Carlinf, R.J. Charity, R.T. de Souza[e], C.K. Gelbke[a], W.C. Hsi[ae], G.J. Kunde[ad], M-C. Lemaire[b], M.A. Lisa[a], U. Lynen[d], G.F. Peaslee[a], J. Pochodzalla[d], H. Sann[d], L.G. Sobotka[c], S.R. Souza[b], and W. Trautmann[d]

[a] *NSCL and Department of Physics and Astronomy, Michigan State University, East Lansing, MI 48824, USA.* [b] *Laboratoire National SATURNE, CEN Saclay, 91191 Gif-sur-Yvette Cedex, France.* [c] *Department of Chemistry, Washington University, St. Louis, MO 63130, USA.* [d] *Gesellschaft für Schwerionenforschung, D-6100 Darmstadt 11, Germany.* [e] *IUCF and Department of Chemistry, Indiana* University, Bloomington, *IN 47405, USA.* [f] *Instituto de Fisica, Universidade de São Paulo, CEP 01498, São Paulo, Brazil.*

Abstract

Sidewards directed fragment flow has been extracted for $^{84}Kr+^{197}Au$ collisions at E/A=200 MeV, wing techniques that are free of reaction plane dispersion. The fragment flow per nucleon increases with mass, following a thermal- or coalescence-like behavior, end attains roughly constant limiting values at $4 \leq A \leq 12$. Comparisons of the impact parameter dependences of the measured coalescence-invariant proton flow to Boltzmann-Uehling-Uhlenbeck calculations clearly favor a momentum dependent nuclear mean field.

25.75.+r, 25.70.Pq

The determination of the equation of state (EOS) of nuclear matter is an important objective of nuclear physics. Information about the equation of state can be extracted from the collective flow of nuclear matter deflected sidewards from the hot and dense region formed by the overlap of projectile and target nuclei [1,2]. This flow reflects the interplay of collective and random motions. For a thermalized system, the random motions of emitted fragments are dictated by the thermal energy, which is independent of mass. In contrast, contributions to the fragment energy due to collective motion increase linearly with mass and are more easily observed for heavier fragments [3–5].

Flow measurements confirm that the transverse collective flow of light charged particles (p,d,t,α) increases with mass [3]. Limited studies for Z>2 indicate stronger flow effects for intermediate mass fragments than for light charged particles [5], but a systematic understanding of the mass dependence of collective fragment flow is lacking. Such information is essential for quantitative flow extraction at incident energies E/A$\leq$250 MeV, where fragments remove much of the total mass [6,7]. In this letter we perform a quantitative investigation of the mass dependence of directed collective flow which includes intermediate mass fragments up to Z=6. We explore these effects with the mass-asymmetric ^{84}Kr+ ^{197}Au system which allows clear distinctions between different parametrization of the nuclear EOS.

In the experiment, 5 mg/cm^2 thick ^{197}Au targets were bombarded with 200A MeV ^{84}Kr beams of the Laboratoire National SATURNE at Saclay. The emitted charged particles were detected with 276 low-threshold plastic-scintillator-CsI(Tl) phoswich detectors of the combined Miniball/ Wall array [8], which covered 90% of 4π in solid angle. Unit charge resolution beyond Z$\sim$12 was routinely achieved for particles which stopped in the CsI(Tl) scintillators. Ball detectors at backward angles, θ_{lab}= 25°-160°, incorporated 4 mg/cm^2 scintillator foils and 2 cm thick CsI(Tl) crystals and had particle identification (PID) thresholds of E_{th}/A $\sim$2

(4) MeV for Z=3 (10) particles, respectively. Wall detectors at forward angles, θ_{lab}=5.4°-25°, incorporated 8 mg/cm^2 foils and 3 cm thick CsI(Tl) crystals and had PID thresholds of 4 (6) MeV for Z=3 (10) particles, respectively. Flow analyses were performed within an energy gate of E/A = 20-75 MeV which took the minimum energy for ^{3}He and α separation and the range for energetic protons in the Miniball detectors into account. An impact parameter scale was constructed from the total detected charged particle multiplicity and normalized via cross section measurements [6]. Further details about the experiment can be found in Ref. [6].

The in-plane component of the directed flow is usually extracted by techniques [9], wherein the momenta of detected particles are projected onto an experimentally determined reaction plane . At incident energies of E/A$\approx$ 200 MeV, techniques for locating this reaction plane utilize asymmetries in the emission patterns of particles which originate from their deflection from the compressed overlap region between projectile and target nuclei. Experimentally extracted reaction planes generally fluctuate about the true reaction plane for each event [10], however, introducing uncertainties in the extracted transverse momenta. Corrections for this reaction plane dispersion may be applied, but have uncertainties that become especially large when the flow is weak [11].

To avoid such uncertainties, we have followed the techniques of ref. [12] wherein the inner product $p_\nu^\perp(y_\nu) \cdot p_\mu^\perp(y_\mu)$ between the transverse momentum $p_\nu^\perp(y_\nu)$ of a particle of type ν at rapidity y_ν and the transverse momentum $p_\mu^\perp(y_\mu)$ of a particle of type μ at rapidity y_μ is averaged over the transverse momenta of the two particles. Random fluctuations of the transverse momenta about the collective mean values then average to zero in this approach, leaving only the collective mean values. Choosing a coordinate system in which the non-vanishing mean collective transverse momenta lie along the x axis, this average inner product becomes [12]:

$$\langle p_\nu^\perp(y_\nu) \cdot p_\mu^\perp(y_\mu)\rangle \simeq \langle p_\nu^x(y_\nu)\rangle\langle p_\mu^x(y_\mu)\rangle. \quad (1)$$

Momentum conservation gives rise to further correlations between particle transverse momenta, modifying Eq. (1) to become [12]:

$$\langle p_\nu^\perp(y_\nu) \cdot p_\mu^\perp(y_\mu)\rangle \simeq \langle p_\nu^x(y_\nu)\rangle\langle p_\mu^x(y_\mu)\rangle - \alpha\langle p_\nu^{\perp^2}(y_\nu)\rangle\langle p_\mu^{\perp^2}(y_\mu)\rangle \quad (2)$$

where $\alpha^{-1} \simeq \langle \sum_\mu p_\mu^{\perp^2}\rangle$ [12] and the sum runs over all emitted particles. (Since the experimental detection efficiency in the present experiment is less than one, the value for α^{-1} used in Eq. (2) was obtained by rescaling the experimental value for α^{-1} by the ratio of the total to the detected mass [13].) Final state interactions and apparatus non-uniformities can influence the extraction of the mean transverse momenta [12]; corrections have been made for these effects following ref. [12] but make little difference to the final results presented here.

Mean two-fragment inner products $\langle p_\nu^\perp(y_\nu) \cdot p_\mu^\perp(y_\mu)\rangle$ were then constructed for each possible pair of particle types with $1 \leq Z_1, Z_2 \leq 6$ and selected bins of normalized rapidity, $y_n = y_{cm}/y_{beam}$. Eq. (2) was then solved by matrix diagonalization to obtain initial values for $\langle p_\nu^x(y_\nu)\rangle$ in the different rapidity bins [12]. Final values for $\langle p_\nu^x(y_\nu)\rangle$ were obtained by a least squares minimization procedure in which the $\langle p_\nu^x(y_\nu)\rangle$ on the r.h.s. of Eq. (2) were varied from their initial values so as to accurately satisfy Eq. (2). This procedure permitted an assessment of the uncertainties in the values for $\langle p_\nu^x(y_\nu)\rangle$.

Data were analyzed for two distinct impact parameter gates: $1 \leq b \leq 3$ fm and $4 \leq b \leq 6$ fm. Within these gates, analyses were performed for particles with $-0.2 \leq y_n \equiv y/y_{beam} \leq 0.2$ in the center of momentum (c.m.) frame. As illustrated for Beryllium fragments in Fig. 1(a), flow values in this rapidity interval are not significantly distorted by the Miniball acceptance. (Further details of these simulations are given below.) Measured mean transverse momenta per nucleon $\langle p^x/A\rangle$, shown in Fig. 1(b) for protons and Beryllium fragments at $4 \leq b \leq 6$

fm, reveal enhanced transverse momenta for heavier particles, consistent with trends observed in previous studies [3,5]. Near $y_n = 0$, the data in Fig. 1(b) are well characterized by the collective flow, $F = d\langle p^x/A\rangle/dy_n$, which can be easily extracted via a linear least-squares fit near mid-rapidity. The flow per nucleon, $d\langle p^x/A\rangle/dy_n$, shown as a function of fragment mass in Fig. 2 for the two impact parameter gates, is larger for the more peripheral gate. Consistent with previous measurements [3,5,14], the flow increases strongly with mass for Z$\leq$2, but becomes roughly independent of mass for heavier fragments.

To determine whether these features may arise from the interplay between collective and thermal motion, we have simulated the velocity distributions of the fragments with a thermal expression of the form

$$P(\mathbf{v}) = \int d\mathbf{v}\mathcal{F}(\mathbf{v}_{coll})\mathcal{G}(\mathbf{v}_{th})\delta(\mathbf{v} - \mathbf{v}_{coll} - \mathbf{v}_{th}). \quad (3)$$

Here, we assume a collective velocity distribution of Gaussian form $\mathcal{F}(\mathbf{v}_{coll}) \propto \exp(-\sum_i [\mathbf{v}^i_{coll}]^2/2\sigma_i^2)$ with three independent principal axes to approximate the situation before breakup. We further assume that the momenta of the produced particles obtain additional random velocity components according to the distribution $\mathcal{G}(\mathbf{v}_{th}) \propto \exp(-A\mathbf{v}^2_{th}/2T)$, where A is the fragment mass number and T is a temperature parameter. The principal axes of the collective velocity distribution are rotated by the flow angle, θ_F; σ_3 characterizes the distribution along the flow axis and σ_1 and σ_2 characterizes the other widths in and perpendicular to the reaction plane, respectively. These values for σ_i and T were adjusted to reproduce the measured rapidity and transverse energy distributions. The solid (dashed) line in Fig. 2, for calculations assuming $\sigma_1 = \sigma_2 = 0.1c, \sigma_3 = 0.15c, \theta_F = 55°$, $T = 55$ MeV ($\sigma_1 = \sigma_2 = 0.1c, \sigma_3 = 0.16c, \theta_F = 55°$, $T = 45$ MeV), reproduces everything but the α particle data, for which small relative momentum correlations reveal strong contaminations from secondary decays of heavier fragments with large flow values. While this parameterization is not unique, the model indicates

that the near constancy of the heavy fragment flow occurs because it is primarily governed by the collective velocity distribution. The flow for light particles is then reduced relative to that for heavy fragments due to a mass dependent thermal mixing between the collective velocity distributions at positive and negative rapidities in the c.m. system.

In the limit of local thermal equilibrium, coalescence and thermodynamic models make very similar predictions for the particle mass dependence of momentum distributions [15]. The level of agreement shown in Fig. 2 therefore implies consistency with coalescence-like cluster production mechanisms [16] and provides a justification for coalescence-invariant analyses. Accordingly we constructed a coalescence-invariant effective proton flow

$$F_{eff} = \sum Z_i Y_i F_i / \sum Z_i Y_i, \tag{4}$$

where the Z_i, Y_i, and F_i are the charge, yield, and flow values for the various particle species, to enable comparisons to the proton flow predicted by transport models such as the Boltzmann-Uehling-Uhlenbeck (BUU) equation and render comparisons to molecular dynamics models which do not accurately describe the fragment observables [6] unnecessary. If one constructs the effective proton flow using the measured flow and yield data for Z$\leq$ 6 one obtains 51$\pm$11 and 89$\pm$10 MeV/c for 1$<$ b$<$ 3 and 4$<$ b$<$ 6, respectively. Using the measured charge yields and Eq. 3 to extrapolate from $Z \leq 6$ to $Z \leq 12$ raises the corresponding flow values to 54$\pm$11 and 92$\pm$10 MeV/c, respectively. These two extrapolated experimental effective proton flow values plus a similarly constructed overlapping intermediate value for 2.5$<$ b$<$ 4.5 are plotted in Fig. 3 as the cross-hatched rectangles with horizontal widths that represent the relevant impact parameter bins and vertical widths (uncertainties) that primarily reflect an estimated ($<$ $1fm$) uncertainty in the determination of the average impact parameter. Note that the effective proton flow exceeds the measured proton flow, as expected

for the coalescence model which creates clusters and depletes free proton flux in densely occupied regions in phase space, where collective phenomena are most strongly manifested.

To test the sensitivity of this measurement to the transport parameters, BUU calculations have been performed for various parametrizations of the mean field potential and including a nucleon-nucleon cross section which has been parameterized to describe measured nucleon-nucleon scattering data [17]. These calculations are shown in Fig. 3 for a soft (K=200 MeV) mean field (**SM** - open diamonds) and a hard (K=386 MeV) mean field (**HM** - solid diamonds) with a momentum dependence consistent with non-locality effects observed in nucleon-nucleus potential scattering [18]. Calculations with a soft mean field (**S** - open squares) and a hard mean field (**H** - open circles) without momentum dependence are also shown. All calculations have been impact parameter averaged and filtered by the experimental acceptance.

Calculations indicate that mean field repulsion (nucleon-nucleon collisions) governs the flow for the momentum dependent (independent) simulations [19]. These differences cause alterations to the time dependent non-equilibrium transport that provide the differences in impact parameter dependences shown in Fig. 3 [20]. The trends of the momentum dependent calculations are in better agreement with experimental data, consistent with investigations at higher incident energies [21–23]. The sensitivity to the compressibility parameter K is slight, however. Improved agreement between the momentum dependent calculations and the data can be obtained by a 20% density dependent reduction of the in-medium nucleon-nucleon cross section of the form $\sigma_{NN} = (1 - 0.2\frac{\rho}{\rho_o})\sigma_{free}$ [24], consistent with the systematics of the disappearance of collective flow [24] and with microscopic calculations of the in-medium corrections to the nucleon-nucleon cross section [25], This is illustrated by the solid circles in the Fig. 3 for a soft momentum dependent mean field (**SM** $(\mathbf{0.8}\sigma_{free})$).The calculations

with reduced cross section are somewhat higher than the data. These discrepancies can only be reduced by a few percent by including the presently uncounted contributions to the effective proton flow from fragments with Z> 12.

In summary, we have measured the mass dependence of sidewards directed collective flow for the system ^{84}Kr+^{197}Au at an incident energy of 200 MeV/A, where fragments carry a significant fraction of the mass and the collective flow. The flow has a linear mass dependence for light fragments, but is nearly independent of mass for intermediate mass fragments with Z>2. With the exception of α particles, the mass dependence is reproduced by model calculations which superimpose a thermal velocity distribution upon a collective velocity distribution. These calculation suggests that the flow of heavy fragments is governed mainly by the collective velocity distribution. Comparisons to BUU calculations demonstrate a definite preference for a momentum dependent mean field and offer support for a 20% density dependent reduction in the nucleon-nucleon cross-section from the value in free space.

This work is supported by the National Science Foundation under Grants No. PHY-90-15255, PHY-92-14992, and PHY-94-03666 and the U.S. Department of Energy under Contract No. DE-FG02-87ER-40316. W.G.L and L.G.S. acknowledge the receipt of U.S. Presidential Young Investigator Awards. W.B. acknowledges support from the U.S. NSF PFF program. N. Carlin and S.R. Souza acknowledge partial support by the CNPq, Brazil. We gratefully acknowledge the support and hospitality extended to us during our experiment at the LNS.

REFERENCES

[1] H.H. Gutbrod, A.M. Poskanzer and H.G. Ritter, Rep. Prog. Phys., **52,** 1267 (1989) and refs. therein.

[2] H. Stöcker and W. Greiner, Phys. Rep., **137,** 277 (1986) and refs. therein.

[3] M.D. Partlan *et al.*, Phys. Rev. Lett. **75**, 2100 (1995).

[4] S.C. Jeong *et al.*, Phys. Rev. Lett. **72**, 3468 (1994).

[5] K.G.R. Doss *et al.*, Phys. Rev. Lett. **59**, 2720 (1987); H.Å. Gustafsson *et al.*, Mod. Phys. Lett. **A3**, 1323 (1989).

[6] G. Peaslee *et al.*, Phys. Rev. C **49**, R2271 (1994).

[7] M. B. Tsang et al., Phys. Rev. Lett. **71**, 1502 (1993).

[8] R.T. de Souza et al, Nucl. Instr. Meth. A 295, 109 (1990); The Miniwall, a granular extension of the Miniball to forward angles, uses the readout technology of D.W. Stracener et al, Nucl. Inst. Meth. A 294, 485 (1990).

[9] P. Danielewicz and G. Odyniec, Phys. Lett. **157B**, 146 (1985).

[10] Here, the reaction plane is defined to be perpendicular to the total angular momentum.

[11] J.P. Sullivan and J. Péter, Nucl. Phys. **A540**, 275 (1992).

[12] P. Danielewicz *et al.*, Phys. Rev. C **38**, 120 (1988).

[13] This ratio was of order 0.3, but varied with impact parameter [6]. Recoil corrections are small.

[14] S. Wang *et al.*, Phys. Rev. Lett. **74**, 2646 (1995).

[15] L.P. Csernai and J.I. Kapusta, Phys. Rep. **131,** 223 (1986) and refs. therein.

[16] P. Danielewicz and G.F. Bertsch, Nucl. Phys. **A533**, 712 (1991).

[17] D. Klakow, G. Welke, and W. Bauer, Phys. Rev. **C48**, 1982 (1993).

[18] C. Gale et. al., Phys. Rev. **C41**, 1545 (1990).

[19] J. Zhang *et al.*, Phys. Rev. **C50**, 1617 (1994).

[20] F. Daffin *et al.*, in preparation.

[21] C. Gale et al., Phys. Rev. **C35,** 1666 (1987).

[22] J. Aichelin et al., Phys. Rev. Lett. **58**, 1926 (1987).

[23] Q. Pan and P. Danielewicz, Phys. Rev. Lett. **70**, 2062, 3523 (1993).

[24] G.D. Westfall et al., Phys. Rev. Lett. **71**, 1986 (1993).

[25] T. Alm, Nucl. Phys. **A587**, 815 (1995).

FIG. 1.(a) Simulations for the transverse momenta of Beryllium fragments within the thermal model of Eq. 3. Open and filled circles depict calculations with the model before and after corrections for the experimental acceptance have been applied. (b) Measured mean transverse momenta for p and Beryllium fragments at 4<b<6 fm.

FIG. 2. Mass dependence of the collective sidewards flow per nucleon in the reaction plane, $d\langle p_x/A\rangle/dy_n$ for the two impact parameter gates used in the analysis. Here we assume A=2Z for A> 4, where mass identification was not achieved. The solid and dashed lines show the corresponding calculations with the thermal model of Eq.3.

FIG. 3. The cross-hatched rectangles depict the measured effective proton flow. Also shown are the corresponding BUU calculations for the following parameter sets: **H** - hard EOS without momentum dependence (open circles), **S** - soft EOS without momentum dependence (open squares), **HM** - hard EOS with momentum dependence (solid diamonds), **SM** - soft EOS with momentum dependence (open diamonds). **SM** ($\mathbf{0.8\sigma_{free}}$) - soft EOS with momentum dependence and a 20% reduction in the nucleon-nucleon cross-section (solid circles). The theoretical error bars are purely statistical.

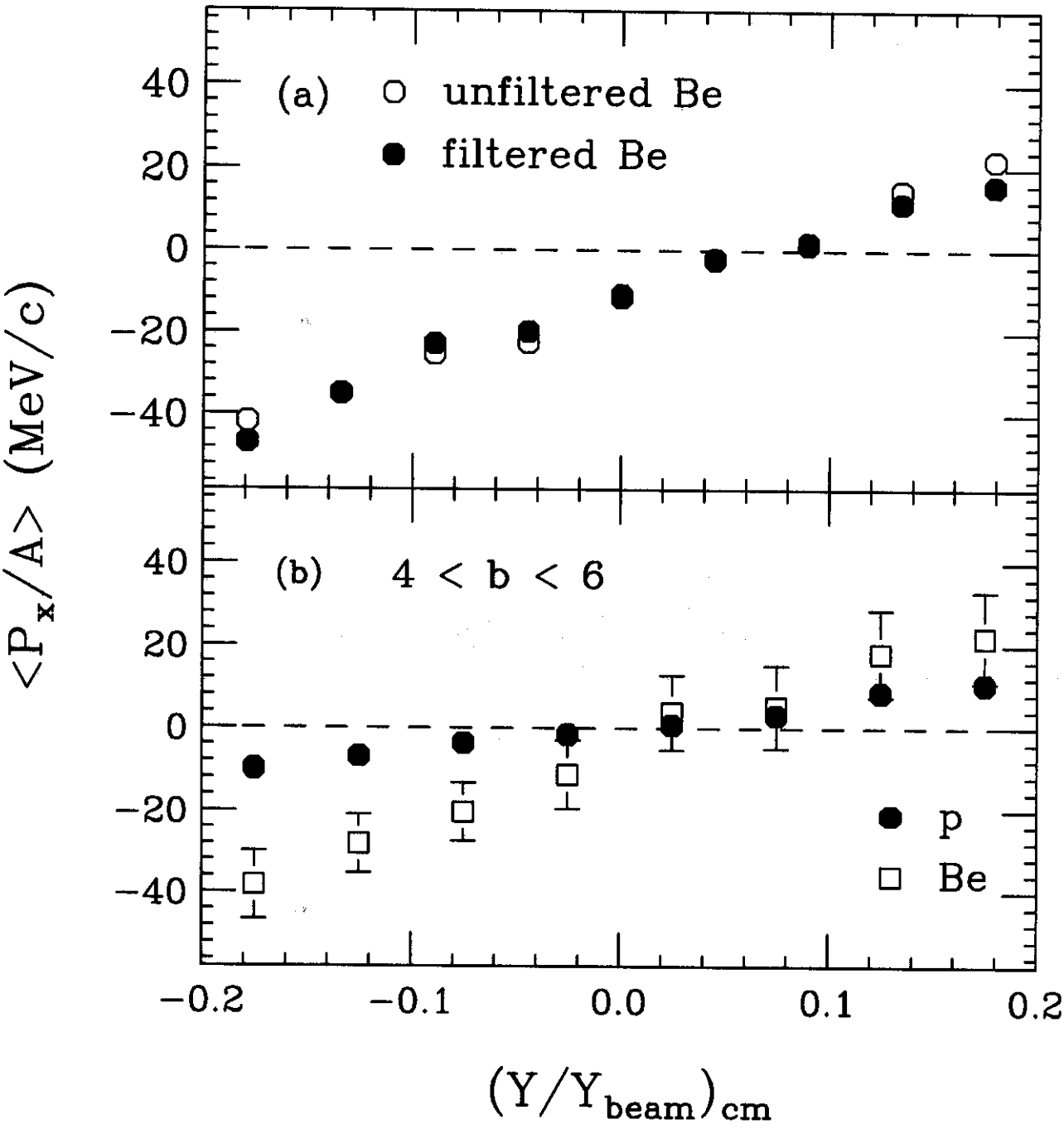
(a) unfiltered Be
filtered Be
(b) 4 < b < 6
p
Be
40
20
0
−20
−40
−0.2
−0.1
0.0
0.1
0.2
$\langle P_x/A \rangle$ (MeV/c)
$(Y/Y_{beam})_{cm}$

Fig. 1

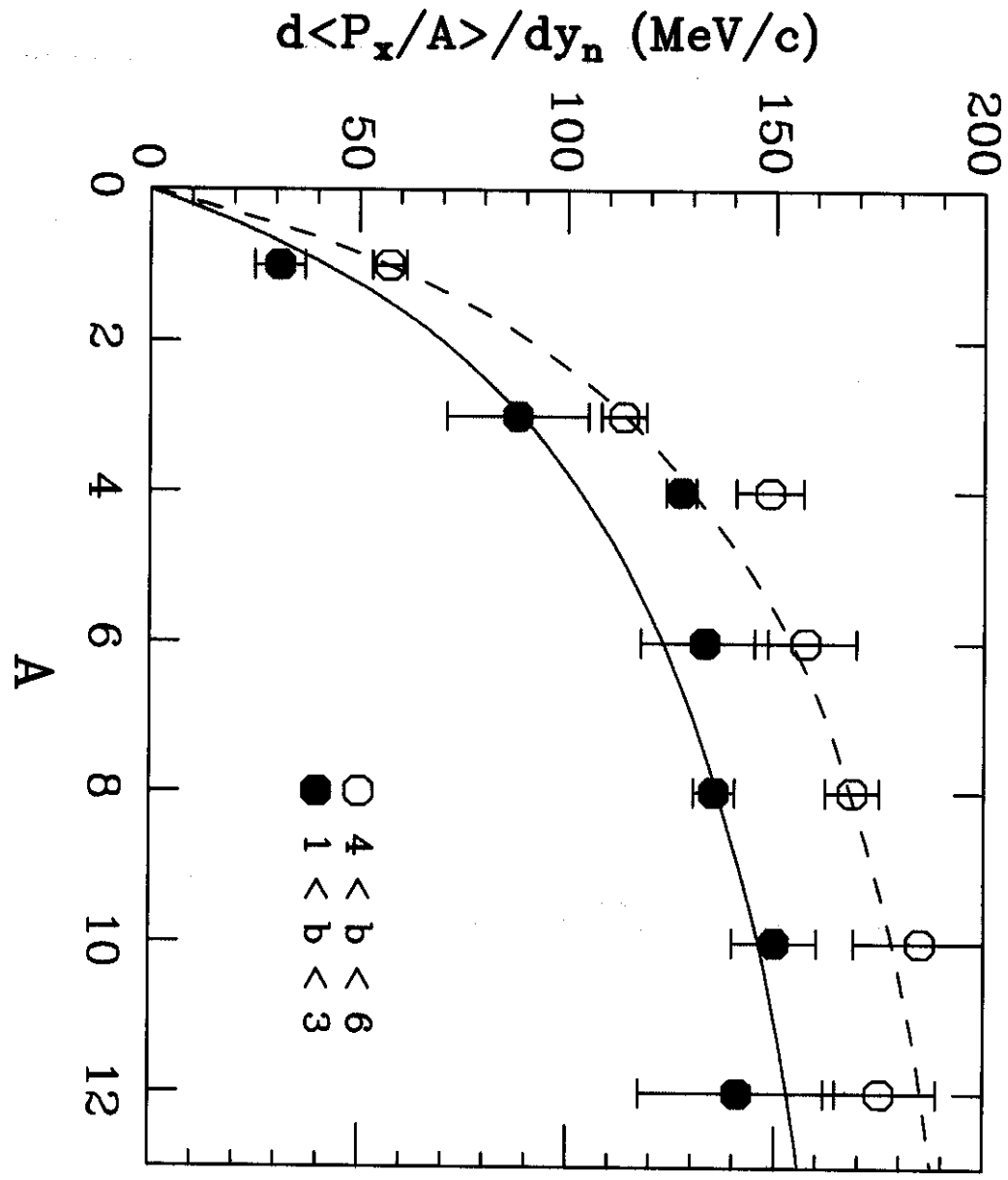

Fig. 2

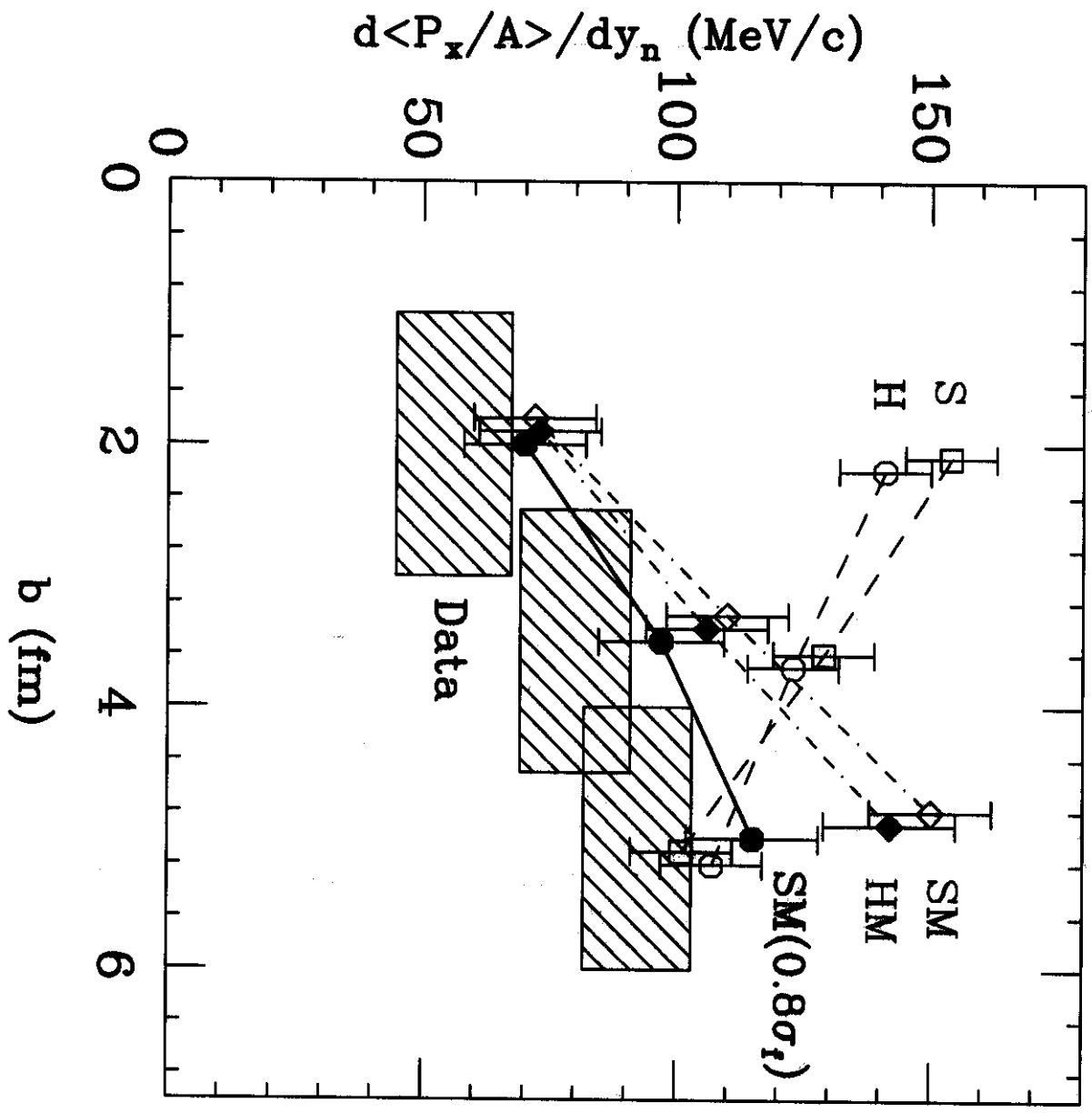

Fig.3